Article

Highly Sensitive and Selective Colorimetric Sensors for Uranyl (UO): Development and Comparison of Labeled and Label-Free DNAzyme-Gold Nanoparticle Systems

Jung Heon Lee, Zidong Wang, Juewen Liu, and Yi Lu

J. Am. Chem. Soc., **2008**, 130 (43), 14217-14226 • DOI: 10.1021/ja803607z • Publication Date (Web): 07 October 2008

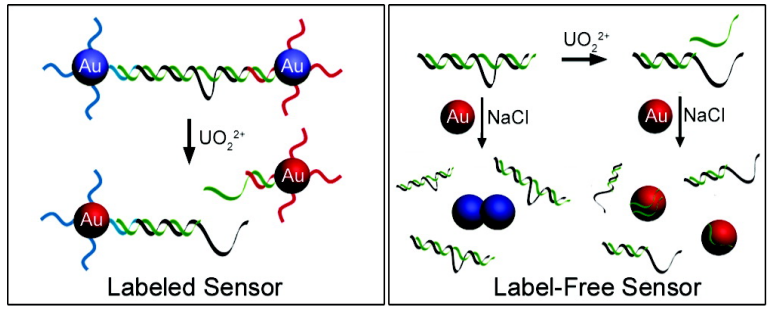

More About This Article

Additional resources and features associated with this article are available within the HTML version:

- Supporting Information
- Access to high resolution figures
- Links to articles and content related to this article
- Copyright permission to reproduce figures and/or text from this article

View the Full Text HTML

J|A|C|S
ARTICLES

Published on Web 10/07/2008

Highly Sensitive and Selective Colorimetric Sensors for Uranyl (UO_2^{2+}): Development and Comparison of Labeled and Label-Free DNAzyme-Gold Nanoparticle Systems

Jung Heon Lee,[†,§] Zidong Wang,[†,§] Juewen Liu,[‡,§] and Yi Lu*[,†,‡,§]

Department of Materials Science and Engineering, Department of Chemistry, and Beckman Institute for Advanced Science and Technology, University of Illinois at Urbana−Champaign, Urbana, Illinois 61801

Received May 14, 2008; E-mail: yi-lu@illinois.edu

Abstract: Colorimetric uranium sensors based on uranyl (UO_2^{2+}) specific DNAzyme and gold nanoparticles (AuNP) have been developed and demonstrated using both labeled and label-free methods. In the labeled method, a uranyl-specific DNAzyme was attached to AuNP, forming purple aggregates. The presence of uranyl induced disassembly of the DNAzyme functionalized AuNP aggregates, resulting in red individual AuNPs. Once assembled, such a "turn-on" sensor is highly stable, works in a single step at room temperature, and has a detection limit of 50 nM after 30 min of reaction time. The label-free method, on the other hand, utilizes the different adsorption properties of single-stranded and double-stranded DNA on AuNPs, which affects the stability of AuNPs in the presence of NaCl. The presence of uranyl resulted in cleavage of substrate by DNAzyme, releasing a single stranded DNA that can be adsorbed on AuNPs and protect them from aggregation. Taking advantage of this phenomenon, a "turn-off" sensor was developed, which is easy to control through reaction quenching and has 1 nM detection limit after 6 min of reaction at room temperature. Both sensors have excellent selectivity over other metal ions and have detection limits below the maximum contamination level of 130 nM for UO_2^{2+} in drinking water defined by the U.S. Environmental Protection Agency (EPA). This study represents the first direct systematic comparison of these two types of sensor methods using the same DNAzyme and AuNPs, making it possible to reveal advantages, disadvantages, versatility, limitations, and potential applications of each method. The results obtained not only allow practical sensing application for uranyl but also serve as a guide for choosing different methods for designing colorimetric sensors for other targets.

Introduction

Uranium is a radioactive metal that exists ubiquitously in the environment.[1] Since uranium is one of the main sources in nuclear energy generation and enriched uranium is a major component in nuclear weapons, human beings have a high chance of being exposed to uranium, which can cause severe adverse effects to human health.[2,3] For these reasons, detection of uranium is very important. However, current analytical techniques, such as inductively coupled plasma, atomic absorption spectrometry, and phosphorimetry all require expensive and complicated instruments, making on-site real-time sensing difficult.[4−7] Toward portable metal ion sensors, remarkable progresses have been made on the design of sensors using various techniques including fluorescence,[8−17] surface plasmon resonance,[18] electrochemistry,[19−21] and colorimetry.[22−25] Despite the progress, there are only a few reported sensors specific

[†] Department of Materials Science and Engineering.
[§] Beckman Institute for Advanced Science and Technology.
[‡] Department of Chemistry.

(1) Gongalsky Konstantin, B. *Environ. Monit. Assess.* **2003**, *89*, 197–219.
(2) Craft, E.; Abu-Qare, A.; Flaherty, M.; Garofolo, M.; Rincavage, H.; Abou-Donia, M. *J. Toxicol. Environ. Health B Crit. Rev.* **2004**, *7*, 297–317.
(3) Zhou, P.; Gu, B. *Environ. Sci. Technol.* **2005**, *39*, 4435–4440.
(4) Abbasi, S. A. *Int. J. Environ. Anal. Chem* **1989**, *36*, 163–172.
(5) Brina, R.; Miller, A. G. *Anal. Chem.* **1992**, *64*, 1413–1418.
(6) Boomer, D. W.; Powell, M. J. *Anal. Chem.* **1987**, *59*, 2810–2813.
(7) Mlakar, M.; Branica, M. *Anal. Chim. Acta* **1989**, *221*, 279–287.
(8) Li, J.; Lu, Y. *J. Am. Chem. Soc.* **2000**, *122*, 10466–10467.
(9) Burdette, S. C.; Walkup, G. K.; Spingler, B.; Tsien, R. Y.; Lippard, S. J. *J. Am. Chem. Soc.* **2001**, *123*, 7831–7841.
(10) Chen, P.; He, C. *J. Am. Chem. Soc.* **2004**, *126*, 728–729.
(11) Yang, L.; McRae, R.; Henary, M. M.; Patel, R.; Lai, B.; Vogt, S.; Fahrni, C. J. *Proc. Natl. Acad. Sci. U.S.A.* **2005**, *102*, 11179–11184.
(12) Yoon, S.; Albers, A. E.; Wong, A. P.; Chang, C. J. *J. Am. Chem. Soc.* **2005**, *127*, 16030–16031.
(13) Nolan, E. M.; Lippard, S. J. *J. Am. Chem. Soc.* **2007**, *129*, 5910–5918.
(14) Wegner, S. V.; Okesli, A.; Chen, P.; He, C. *J. Am. Chem. Soc.* **2007**, *129*, 3474–3475.
(15) Tsien, R. Y. In *Fluorescent Chemosensors for Ion and Molecule Recognition*; American Chemical Society: Washington, DC, 1993; pp 130−146.
(16) Jiang, P.; Guo, Z. *Coord. Chem. Rev.* **2004**, *248*, 205–229.
(17) Lim, M. H.; Lippard, S. J. *Acc. Chem. Res.* **2007**, *40*, 41–51.
(18) Homola, J.; Piliarik, M. *Springer Ser. Chem. Sens. Biosens.* **2006**, *4*, 45–67.
(19) Xiao, Y.; Lubin, A. A.; Heeger, A. J.; Plaxco, K. W. *Angew. Chem., Int. Ed.* **2005**, *44*, 5456–5459.
(20) Li, D.; Yan, Y.; Wieckowska, A.; Willner, I. *Chem. Commun.* **2007**, 3544–3546.
(21) Willner, I.; Zayats, M. *Angew. Chem., Int. Ed.* **2007**, *46*, 6408–6418.
(22) Elghanian, R.; Storhoff, J. J.; Mucic, R. C.; Letsinger, R. L.; Mirkin, C. A. *Science* **1997**, *277*, 1078–1080.
(23) Liu, J.; Lu, Y. *J. Am. Chem. Soc.* **2003**, *125*, 6642–6643.

for uranium,[26−30] and most of them cannot yet match instrument-based detection in terms of sensitivity and selectivity. A contributing factor in the difficulty of designing sensors for uranium is that uranium has many forms in aqueous solution, and the most soluble or bioavailable form is uranyl (UO_2^{2+}). Unlike most metal ions such as Zn^{2+}, the oxycationic uranyl poses a special challenge for designing a ligand to bind it specifically.

DNA is generally known as a passive genetic informational storage material. In 1994, however, it was reported that DNA with active catalytic functions can been obtained through *in vitro* selection process from a large DNA library, especially in the presence of metal cofactors, and it is thus called catalytic DNA, deoxyribozymes, or DNAzyme.[31] Since then, a number of DNAzymes have been selected that are highly specific for metal ions such as Pb^{2+},[8,31] Cu^{2+},[32−34] Zn^{2+},[35] Co^{2+},[36,37] and Mn^{2+}.[38] Such a selection method has also been shown to be generally applicable to other forms of metal ions, including the oxycation UO_2^{2+}.[39] Recognizing the potential of DNAzymes as a new class of molecules specific for a wide range of metal ions, we and others have converted the DNAzymes into highly sensitive and selective fluorescent sensors using a catalytic beacon method.[8,40−43] For example, recently reported uranyl (UO_2^{2+}) specific DNAzyme fluorescence sensor has a 45 pM detection limit and million-fold selectivity,[39] which rivals those of analytical instruments such as inductively coupled plasma mass spectrometry.

While fluorescent sensors are applicable for accurate on-site and real-time detection of metal ions, they still require portable fluorimeters. Colorimetric sensors gain a lot of interest nowadays since they have the advantage of allowing simple on-site real-time detection without instruments.[44] There are only a few colorimetric sensors reported for uranium,[27,30] but most of them are not selective and have interference with other metal ions. Therefore, developing colorimetric uranium-specific sensors with high sensitivity and selectivity is very important and highly desirable.

Metallic nanoparticles, especially gold nanoparticles (AuNPs), have emerged as a new class of reporters and have received much attention for colorimetric sensing[44−49] due to their high extinction and strong size- and distance-dependent optical properties.[44] The color of the AuNPs is red in dispersed state but changes to blue upon aggregation due to the shift of surface plasmon absorption to a longer wavelength.[47,50] Since the plasmon peak shift of 13 nm AuNP can be directly observed by the naked eye even with the concentration as low as a few nM, the AuNP can be ideally used as a reporter in colorimetric sensing. Especially when combined with DNA, AuNPs have been shown to be very useful for detecting a broad range of molecules, because DNA not only has molecular recognition functions[31,51] but also can control the assembly and disassembly status of AuNPs, in result tuning their optical properties.[46,47,52]

The DNA-based AuNPs colorimetric sensors can be generally classified as either labeled or label-free sensors. The labeled method attaches DNA, DNAzymes, or aptamers onto AuNPs before sensing operation and relies on directed disassembly (or assembly) of AuNPs due to analyte-specific cleavage or conformational change of the DNA molecules. Since AuNPs are highly negatively charged due to the phosphate backbone of DNA, AuNP aggregation can be prevented even in 2.5 M NaCl, while the bare AuNPs are relatively less stable and form aggregates due to the salt-induced screening effect.[49] However, in the presence of the bridging DNA which is complementary to both DNA strands functionalized to AuNPs, AuNPs can be aggregated and the color of AuNPs changes from red to purple due to the plasmon peak shift.[47] Using this phenomenon, DNA-labeled sensors have been reported that can detect DNA,[22,24] protein,[53,54] small molecules,[25] and metal ions.[23,55−58] Such a method has been converted into dip stick format,[59] making it even more simple and straightforward to use.

The label-free colorimetric sensors do not require any attachment of DNA onto AuNPs for the method to work and utilize different adsorption properties of single-stranded (ssDNA) and double-stranded DNA (dsDNA) on citrate-coated AuNPs that affect salt (often NaCl)-induced aggregation of AuNPs.[60]

(24) Hazarika, P.; Ceyhan, B.; Niemeyer, C. M. *Angew. Chem., Int. Ed.* **2004**, *43*, 6469–6471.
(25) Liu, J.; Lu, Y. *Angew. Chem., Int. Ed.* **2006**, *45*, 90–94.
(26) Rohwer, H.; Rheeder, N.; Hosten, E. *Anal. Chim. Acta* **1997**, *341*, 263–268.
(27) Sessler, J. L.; Melfi, P. J.; Seidel, D.; Gorden, A. E. V.; Ford, D. K.; Palmer, P. D.; Tait, C. D. *Tetrahedron* **2004**, *60*, 11089–11097.
(28) Blake, R. C.; Pavlov, A. R.; Khosraviani, M.; Ensley, H. E.; Kiefer, G. E.; Yu, H.; Li, X.; Blake, D. A. *Bioconjug. Chem.* **2004**, *15*, 1125–1136.
(29) Safavi, A.; Bagheri, M. *Anal. Chim. Acta* **2005**, *530*, 55–60.
(30) Greene, P. A.; Copper, C. L.; Berv, D. E.; Ramsey, J. D.; Collins, G. E. *Talanta* **2005**, *66*, 961–966.
(31) Breaker, R. R.; Joyce, G. F. *Chem. Biol.* **1994**, *1*, 223–229.
(32) Cuenoud, B.; Szostak, J. W. *Nature* **1995**, *375*, 611–614.
(33) Carmi, N.; Shultz, L. A.; Breaker, R. R. *Chem. Biol.* **1996**, *3*, 1039–1046.
(34) Wang, W.; Billen, L. P.; Li, Y. *Chem. Biol.* **2002**, *9*, 507–517.
(35) Santoro, S. W.; Joyce, G. F.; Sakthivel, K.; Gramatikova, S.; Barbas, C. F. *J. Am. Chem. Soc.* **2000**, *122*, 2433–2439.
(36) Mei, S. H. J.; Liu, Z.; Brennan, J. D.; Li, Y. *J. Am. Chem. Soc.* **2003**, *125*, 412–420.
(37) Bruesehoff, P. J.; Li, J.; Augustine, A. J.; Lu, Y. *Comb. Chem. High Throughput Screening* **2002**, *5*, 327–335.
(38) Wang, Y.; Silverman, S. K. *J. Am. Chem. Soc.* **2003**, *125*, 6880–6881.
(39) Liu, J.; Brown, A. K.; Meng, X.; Cropek, D. M.; Istok, J. D.; Watson, D. B.; Lu, Y. *Proc. Natl. Acad. Sci. U.S.A.* **2007**, *104*, 2056–2061.
(40) Niazov, T.; Pavlov, V.; Xiao, Y.; Gill, R.; Willner, I. *Nano Lett.* **2004**, *4*, 1683–1687.
(41) Rupcich, N.; Chiuman, W.; Nutiu, R.; Mei, S.; Flora, K. K.; Li, Y.; Brennan, J. D. *J. Am. Chem. Soc.* **2006**, *128*, 780–790.
(42) Liu, J.; Lu, Y. *J. Am. Chem. Soc.* **2007**, *129*, 9838–9839.
(43) Liu, J.; Lu, Y. *Angew. Chem., Int. Ed.* **2007**, *46*, 7587–7590.
(44) Liu, J.; Lu, Y. *Nat. Protoc.* **2006**, *1*, 246–252.
(45) Zhao, W.; Gonzaga, F.; Li, Y.; Brook, M. A. *Adv. Mater.* **2007**, *19*, 1766–1771.
(46) Storhoff, J. J.; Lazarides, A. A.; Mucic, R. C.; Mirkin, C. A.; Letsinger, R. L.; Schatz, G. C. *J. Am. Chem. Soc.* **2000**, *122*, 4640–4650.
(47) Mirkin, C. A.; Letsinger, R. L.; Mucic, R. C.; Storhoff, J. J. *Nature* **1996**, *382*, 607–609.
(48) Sato, K.; Hosokawa, K.; Maeda, M. *J. Am. Chem. Soc.* **2003**, *125*, 8102–8103.
(49) Lim, I. I.; Ip, W.; Crew, E.; Njoki, P. N.; Mott, D.; Zhong, C. J.; Pan, Y.; Zhou, S. *Langmuir* **2007**, *23*, 826–833.
(50) Lee, J. H.; Wernette, D. P.; Yigit, M. V.; Liu, J.; Wang, Z.; Lu, Y. *Angew. Chem., Int. Ed.* **2007**, *46*, 9006–9010.
(51) Ellington, A. D.; Szostak, J. W. *Nature* **1990**, *346*, 818–822.
(52) Li, H.; Rothberg, L. *Proc. Natl. Acad. Sci. U.S.A.* **2004**, *101*, 14036–14039.
(53) Pavlov, V.; Xiao, Y.; Shlyahovsky, B.; Willner, I. *J. Am. Chem. Soc.* **2004**, *126*, 11768–11769.
(54) Huang, C.-C.; Huang, Y.-F.; Cao, Z.; Tan, W.; Chang, H.-T. *Anal. Chem.* **2005**, *77*, 5735–5741.
(55) Liu, J.; Lu, Y. *J. Am. Chem. Soc.* **2004**, *126*, 12298–12305.
(56) Liu, J.; Lu, Y. *J. Am. Chem. Soc.* **2005**, *127*, 12677–12683.
(57) Lee, J.-S.; Han, M. S.; Mirkin, C. A. *Angew. Chem., Int. Ed.* **2007**, *46*, 4093–4096.
(58) Liu, J.; Lu, Y. *Chem. Commun.* **2007**, 4872–4874.
(59) Liu, J.; Mazumdar, D.; Lu, Y. *Angew. Chem., Int. Ed.* **2006**, *45*, 7955–7959.
(60) Li, H.; Rothberg, L. J. *J. Am. Chem. Soc.* **2004**, *126*, 10958–10961.

AuNPs are inherently not stable and will aggregate out of solution. Most AuNPs are stabilized by a small molecule such as citrate. The presence of salt, however, will decrease citrate's stabilization effects and cause AuNP aggregation. Because ssDNA is flexible and can partially uncoil its bases, it can easily be adsorbed on AuNPs and enhance electrostatic repulsion between AuNPs, which in turn stabilizes AuNPs even in the presence of NaCl.[52,60] On the other hand, as dsDNA is stiff and exposed by a negatively charged phosphate backbone,[61] the strong repulsion between dsDNA and AuNPs makes their binding negligible, causing salt-induced aggregation. On the basis of these phenomena, several designs of label-free based sensors have been developed to detect specific DNA[52] and RNA[62] sequences and potassium ions,[63] mercury ions,[64−66] adenosine,[67] cocaine,[68] and thrombin[69] using aptamers. Detection of Pb^{2+} using DNAzyme based on the label-free method has also been reported.[70,71] Recently, a combination of the two methods, salt-induced aggregation method using AuNPs chemically functionalized with DNA, has also been applied to detect adenosine.[67,72]

Because of its high sensitivity and broad applicability, colorimetric sensors based on DNA and AuNPs have been reported recently numerous times, most of which use either the labeled[22−25,53,54,56,57] or label-free method.[52,62−65,67,69−71] Even though both methods are based on the dispersed and aggregated states of AuNPs, the principles of these two methods are different and so are their general properties. It would be very interesting to compare and contrast the two methods to find out their differences in terms of advantages and disadvantages, versatility, limitations, and potential applications. In addition to offering critical guidance for researchers who want to use the methods, fundamental insight gained from such a comparison is important to advancing both the field of bioanalytical chemistry and the broad field of nanobiotechnology. Because previous publications used different DNA systems, it has been difficult to compare the two methods directly to understand the difference between the two. It is therefore desirable to use the same DNA and AuNPs in both systems to provide a direct comparison of the two methods. Here we report the development and optimization of uranyl colorimetric sensors using both labeled and label-free methods by combining DNAzyme and AuNPs in different ways. Both methods result in highly sensitive and selective colorimetric sensors, with detection limits below that of the maximum contamination level of uranium defined by the U.S. Environmental Protection Agency (EPA). Through the process, the general properties of the two colorimetric sensors are compared in various aspects, making this work the first systematic comparison of these two methods using uranium sensing as an example.

Results and Discussion

Labeled DNAzyme-AuNP Colorimetric Sensor. A uranyl-specific DNAzyme was used to assemble DNA-functionalized AuNPs to form purple-colored aggregates as shown in Figure 1A and B. The substrate strand (39S-L) is elongated on both the 5′ and 3′ ends to hybridize with DNAs functionalized on AuNPs (Arm (5′) and Arm (3′)). After annealing the substrate strand (39S-L), the enzyme strand (39E), and AuNPs functionalized with Arm (5′) and Arm (3′) DNA strands, AuNP aggregate is formed. Heating the system above melting temperature will result in the disassembly of the gold nanoparticle due to dehybridization of the arm strands (Arm (5′) and Arm (3′)) from the substrate strand (39S-L), which are 13 and 14 mer long, respectively (Figure 1A). In the presence of uranyl, however, the substrate strand will be cleaved, which makes 9 base pairs between the cleaved RNA site and 3′ end of the enzyme strand (39E) the weakest linkage in the system. This difference in the melting temperature for samples with or without uranyl can be taken advantage of for uranyl sensing.

The enzymatic cleavage activity of the DNAzyme-AuNP construct was first tested to compare its activity without AuNP attached to the DNAzyme. The activity assay was carried out by labeling 39S-L strands with ^{32}P and running polyacrylamide gel electrophoresis (PAGE) (Figure 1C) with 1 μM uranyl at 300 mM NaCl and 50 mM MES (pH 5.5). The results show that the kinetics in DNAzyme-AuNP aggregates (blue curve) was ~200 times slower than that in solution (black curve). We hypothesized that the significant slow down of activity in the aggregates may be due to steric hindrance of AuNP attached immediately to the DNAzyme arm. Therefore, we inserted a 12A spacer to relieve this steric hindrance (Figure 1A). Interestingly, insertion of a 12A spacer on the 5′ end of Arm (5′) strand and 3′ end of Arm (3′) strand increased the initial cleavage rate by ~71%.

We then measured the melting temperature of these DNAzyme-AuNP aggregates (called A_{12} aggregates) to investigate the temperature at which the colorimetric sensor can operate. The aggregates were prepared as described in the Experimental Section, and were kept at room temperature overnight either in the absence or presence of 2.5 μM of UO_2^{2+}. UV−vis spectrometer was used to monitor the extinction change of the samples at 260 nm. An increase of the extinction indicates the melting of the hybridized DNA. As shown in Figure 1D, in the presence of 300 mM NaCl, the sample with uranyl had a melting temperature of ~47 °C whereas one without uranyl had a higher melting temperature of ~57 °C. Because there is a melting temperature difference of 10 °C between the two samples, heating the samples up to a temperature in between the two, 50 °C for example, will induce disassembly of the aggregates with uranyl but not for the one without uranyl. Even at 30 mM NaCl, which was the lowest salt concentration to allow stable AuNP aggregates, the melting temperature was ~40 °C in the absence of uranyl (Figure S1B, Supporting Information). However, when uranyl is added to the aggregates in the presence of 30 mM NaCl at room temperature, only a small amount of uranyl-induced disassembly could be observed (estimated ~50% of disassembly happened after 30 min) (Figure

(61) Bloomfield, V. A.; Crothers, D. M.; Tinoco, I., Jr. *Nucleic Acids: Structures, Properties, and Functions*; University Science Books: Sausalito, CA, 2000; p 800.
(62) Li, H.; Rothberg, L. *Anal. Chem.* **2005**, *77*, 6229–6233.
(63) Wang, L.; Liu, X.; Hu, X.; Song, S.; Fan, C. *Chem. Commun.* **2006**, 3780–3782.
(64) Liu, C. W.; Hsieh, Y. T.; Huang, C.-C.; Lin, Z. H.; Chang, H.-T. *Chem. Commun.* **2008**, *19*, 2242–2244.
(65) Li, D.; Wieckowska, A.; Willner, I. *Angew. Chem., Int. Ed.* **2008**, *47*, 3927–3931.
(66) Wang, L.; Zhang, J.; Wang, X.; Huang, Q.; Pan, D.; Song, S.; Fan, C. *Gold Bulletin* **2008**, *41*, 37–41.
(67) Zhao, W.; Chiuman, W.; Brook, M. A.; Li, Y. *Chembiochem* **2007**, *8*, 727–731.
(68) Zhang, J.; Wang, L.; Pan, D.; Song, S.; Boey, F. Y.; Zhang, H.; Fan, C. *Small* **2008**, *4*, 1196–1200.
(69) Wei, H.; Li, B.; Li, J.; Wang, E.; Dong, S. *Chem. Commun.* **2007**, *36*, 3735–3737.
(70) Wang, Z.; Lee, J. H.; Lu, Y. *Adv. Mater.* **2008**, *20*, 3263–3267.
(71) Wei, H.; Li, B.; Li, J.; Dong, S.; Wang, E. *Nanotechnology* **2008**, *19*, 095501/1−095501/5.
(72) Zhao, W.; Chiuman, W.; Lam, J. C. F.; McManus, S. A.; Chen, W.; Cui, Y.; Pelton, R.; Brook, M. A.; Li, Y. *J. Am. Chem. Soc.* **2008**, *130*, 3610–3618.

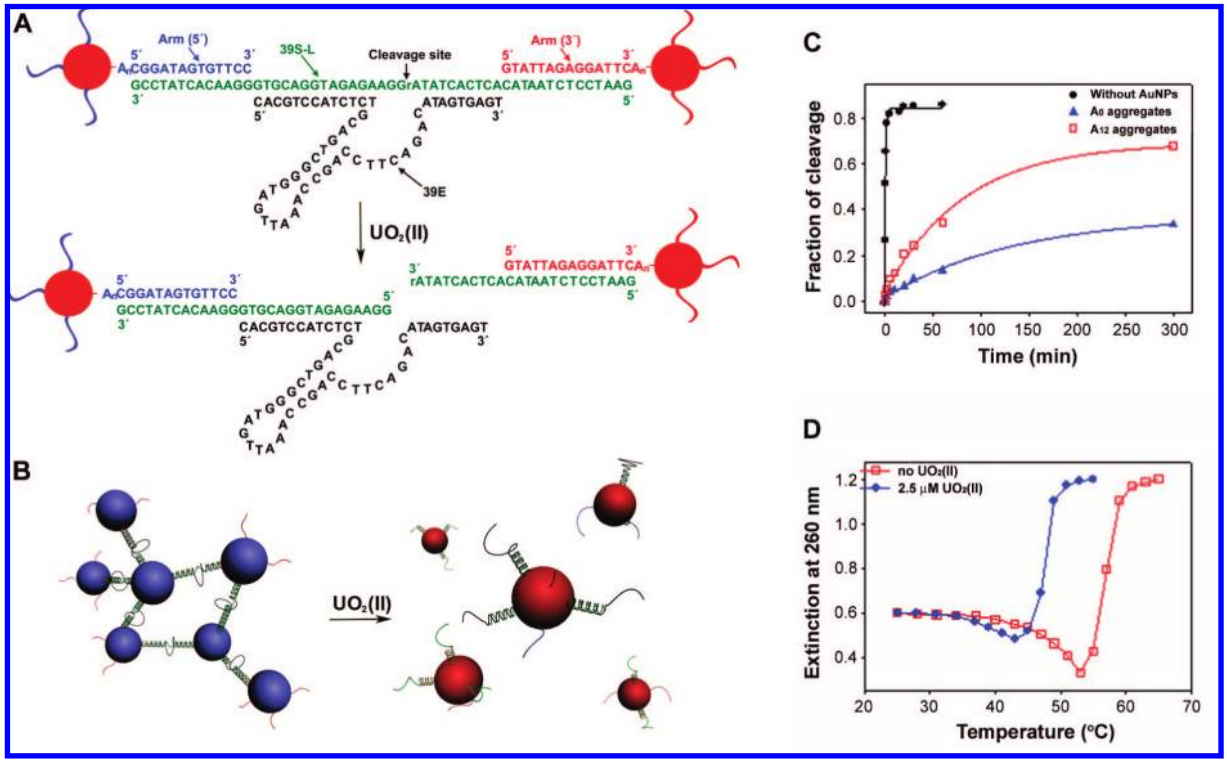

Figure 1. (A) Scheme of labeled colorimetric sensor based on AuNP disassembly in the absence and presence of UO_2^{2+}. In the presence of UO_2^{2+}, the length of the weakest complementary part in the aggregates becomes shorter due to UO_2^{2+}-induced substrate cleavage. The substrate cleavage can decrease the melting temperature of AuNP aggregates. A_n in the arm strands indicates 0A or 12A spacers ($n = 0$ or 12). (B) As UO_2^{2+} is introduced into AuNP aggregates and the temperature is controlled above the melting temperature of UO_2^{2+}-treated aggregates, AuNP disassembles. (C) ^{32}P assay result showing the cleavage kinetics in the presence of UO_2^{2+}. (D) Melting curve of A_{12} aggregates with (blue curve) and without (red curve) UO_2^{2+}. There is about a 10 °C decrease of melting temperature in the presence of UO_2^{2+}. bps = base pairs.

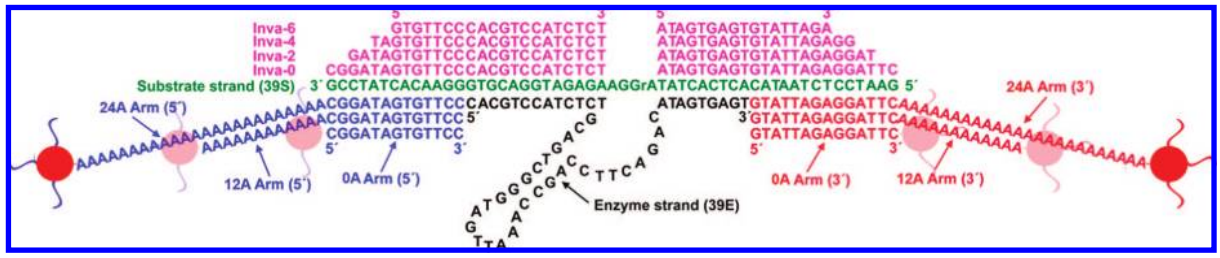

Figure 2. Schematic design of the labeled sensor including the sequences of the invasive DNAs (pink) and 0A, 12A, and 24A Arm strands (blue and red) used in this work.

S2, Supporting Information). Because the disassembly was still too slow, it was necessary to optimize the system to facilitate the disassembly process close to room temperature.

a. Optimization of the Labeled DNAzyme-AuNP System. Because a senor with fast response at room temperature is highly preferred for on-site and real-time operation, invasive DNAs[56] of different lengths (Inva-0, Inva-2, Inva-4, and Inva-6) as well as arm strands with different poly A spacers (0A, 12A, and 24A) were investigated to induce disassembly at room temperature (see Figure 2).

To demonstrate the effect of invasive DNAs on disassembly of AuNPs aggregates, 0A, 12A, 24A, and 36A spacers were investigated in the presence of different invasive DNAs (Figure 3A). A UV−vis spectrometer was used to record the plasmon peak shift of the AuNPs; an integration ratio between 490 to 540 nm and 550 to 700 nm was chosen to monitor the color change (see Supporting Information). The integration between 490 to 540 nm and 550 to 700 nm represents dispersed (ΔD) and aggregated (ΔA) states of AuNPs, respectively.[73] A lower ratio corresponds to aggregation of the AuNPs with blue color whereas a higher ratio corresponds to disperse AuNPs with red color. Because the construct with 36A spacer did not show any color change after aggregation, probably due to the long distance between AuNPs controlled by the length of cross-linking DNA,[46] it was not further investigated.

To investigate the effects of different invasive DNAs on disassembly of AuNP aggregates, the integration ratio (ΔD/ΔA) of AuNP aggregates without poly A spacer (A_0 aggregates) were monitored in the presence of Inva-2, Inva-4, and Inva-6 in the absence of uranyl (Figure 3A) at 40 mM NaCl, 50 mM MES (pH 5.5). Addition of Inva-2, Inva-4, and Inva-6 resulted in integration ratio increase of 0.62, 0.32, and 0.05 after 30 min, respectively, suggesting that invasive DNA-aided AuNP disassembly happens for both Inva-2 and Inva-4, but the extent of

(73) Laromaine, A.; Koh, L.; Murugesan, M.; Ulijn, R. V.; Stevens, M. M. *J. Am. Chem. Soc.* **2007**, *129*, 4156–4157.

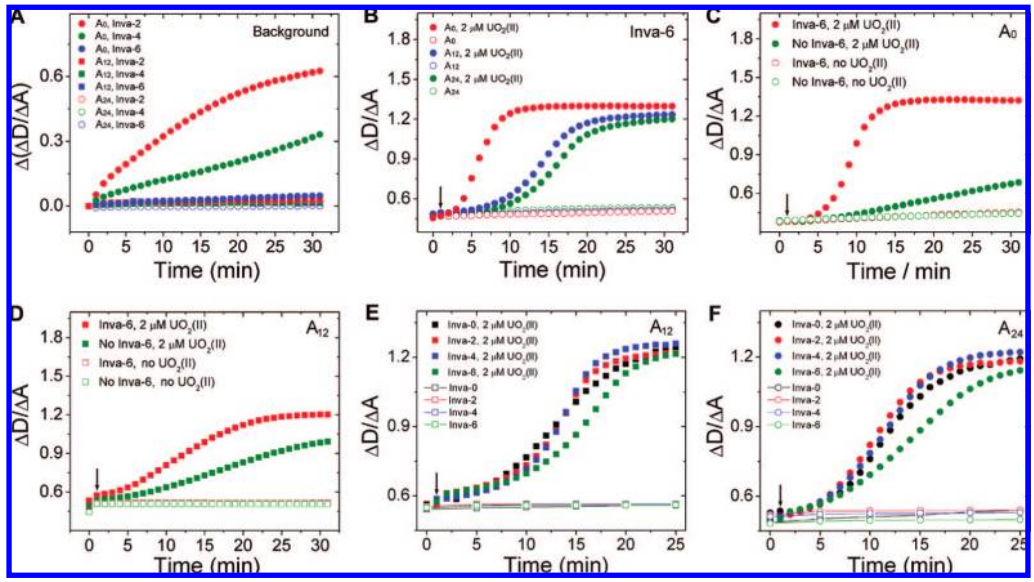

Figure 3. Effects of different invasive DNAs on disassembly of AuNP aggregates. (A) Background increase of A_0, A_{12}, and A_{24} aggregates with invasive DNA strands in the absence of UO_2^{2+}. (B) Disassembly kinetics difference between A_0, A_{12}, and A_{24} aggregates in the presence of Inva-6. The effect of Inva-6 on the UO_2^{2+}-induced disassembly of A_0 (C) and A_{12} (D) aggregates. The effect of longer invasive DNAs on A_{12} (E) and A_{24} (F) aggregates. UO_2^{2+} was added to samples one minute after UV−vis monitoring was started.

disassembly decreases as the length of invasive DNA becomes shorter and becomes negligible for Inva-6. Similar effects of invasive DNA have been observed previously.[56] The same procedure was carried out with AuNP aggregates with 12A spacers (A_{12} aggregates) in the presence of the same invasive DNAs. Surprisingly, the integration ratio increased by only 0.03, 0.02, and 0.01 for Inva-2, Inva-4, and Inva-6, respectively, indicating that little disassembly of AuNPs could be observed for invasive DNA of any length tested. The experiment was repeated with AuNP aggregates with 24A spacers (A_{24} aggregates) with all three invasive DNAs and again, integration ratio increases of only 0.02, 0.02, and 0.002 were observed for Inva-2, Inva-4, and Inva-6, respectively. This shows that invasive DNA-induced disassembly of AuNPs did not happen regardless of the length of invasive DNAs for A_{24} aggregates. Because invasive DNA-induced disassembly of AuNP aggregates increases background, it is preferred to use an invasive DNA causing a smaller extent of disassembly. As Inva-6 shows negligible increase of disassembly not only for A_{12} and A_{24} aggregates but also for A_0 aggregates, we concluded that Inva-6 is the invasive DNA that can be used for all three aggregates with negligible background increase.

Once Inva-6 was determined to be the most suitable invasive DNA, because of its negligible background increase over Inva-2 or Inva-4, we then investigated the effects of spacers with Inva-6 in the presence of 2 μM uranyl (See Figure 3B) at 40 mM NaCl, 50 mM MES (pH 5.5). In the case of A_0 aggregates, the integration ratio started to increase in less than 5 min and was saturated in about 10 min, suggesting that disassembly can be completed in less than 15 min. In contrary, both A_{12} and A_{24} aggregates showed much slower integration ratio increase and saturation at about 20−25 min, meaning that it takes about 25 min for A_{12} or A_{24} aggregates to be disassembled with Inva-6. Surprisingly, it shows that A_0 aggregates disassemble the fastest whereas A_{12} and A_{24} aggregates were both significantly slower with Inva-6. What is observed here differs from the activity assay result shown in Figure 1C which showed that poly A spacers in the arm strands can help uranyl-induced cleavage. This result made us wonder how the combination of the invasive DNA and the spacer in arm strands affects the performance of the sensor, since these two factors were both shown to facilitate the disassembly of the aggregation individually. Is their combination constructive or destructive?

To answer the above question, we compared the performance of the sensor with and without invasive DNA in A_0 aggregates and A_{12} aggregates in the presence of 2 μM uranyl at 40 mM NaCl, 50 mM MES (pH 5.5). In the case of A_0 aggregates, the integration ratio increased very slowly from 0.39 to 0.68 in 30 min in the absence of Inva-6 (Figure 3B). In the presence of Inva-6, however, its integration ratio started to increase from 0.38 in about 4 min after addition of uranyl and was saturated in about 13 min up to the integration ratio of ~1.32, which is about a 224% increase based on the integration ratio response in 30 min (Figure 3C). This result suggests that uranyl-induced disassembly kinetics of A_0 aggregates is significantly increased upon the addition of Inva-6. On the other hand, the integration ratio of A_{12} aggregates increased from ~0.49 to 0.99 after 30 min of reaction, which is approximately 2 times the integration increase of A_0 aggregates in the absence of Inva-6 (Figure 3D). However, even though Inva-6 is added to A_{12} aggregates, the integration ratio only increased from 0.53 to 1.2 and saturation happened in about 25 min. This shows that even though Inva-6 helps to disassemble Au_{12} aggregates, it induces only a 34% increase based on the integration ratio after 30 min of reaction, which is much lower than A_0 aggregates (224%). Therefore we conclude that Inva-6 works the most effectively with A_0 aggregates and its contribution in A_0 aggregates is more significant than that from A_{12} or A_{24} aggregates.

Considering the fact that Inva-6 was able to accelerate the disassembly more effectively in the A_0 aggregate than in the A_{12} and A_{24} aggregates, the possible reason might be lower activation energy necessary to replace arm strands. When AuNP are functionalized to arm strands without spacers, the stability of substrate strand and both arm strand duplexes (5′ and 3′) would be impaired and thus vulnerable to the attacking by invasive DNA due to the electrostatic repulsion between NPs, steric hindrance, and nonspecific adsorption of ssDNA strand

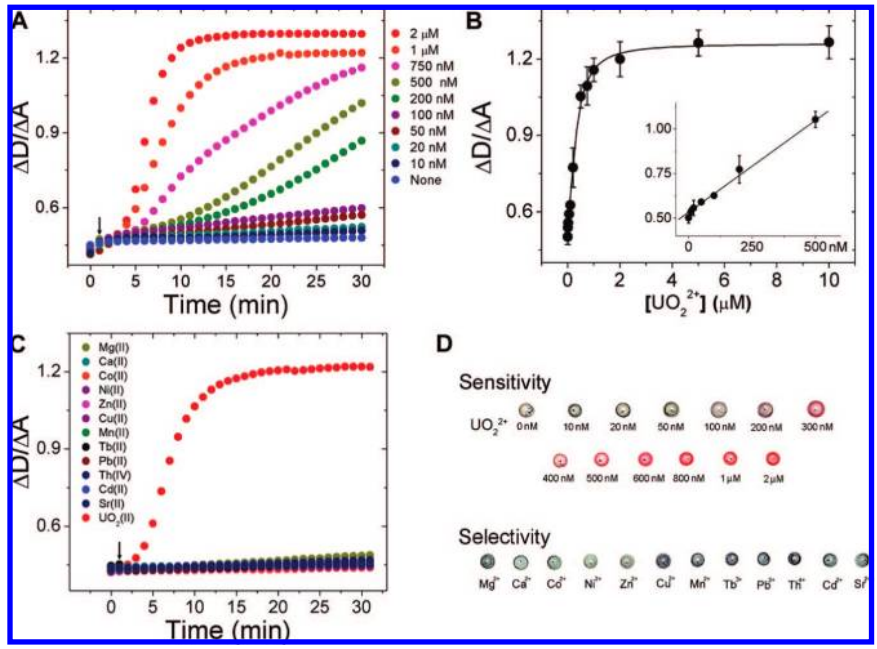

Figure 4. (A) Effects of different invasive DNAs on disassembly of AuNP aggregates. (A) Disassembly of AuNP aggregates at various UO_2^{2+} concentrations and (B) calibration curve of labeled uranyl colorimetric sensor. (C) Disassembly of AuNPs in the presence of various metal ions including UO_2^{2+}. (D) Color change of AuNP aggregates in the presence different concentrations of UO_2^{2+} and other metal ions. The concentration of all metal ions other than UO_2^{2+} is 2 μM. Metal ions were added to samples one minute after UV−vis monitoring was started.

on AuNP surface.[46,47,74] For comparison, in the case of A_{12} and A_{24} aggregates, it contains 12A and 24A spacers, respectively, which can minimize the destabilization of the duplex caused by AuNPs. Because the substrate strand and complementary arm strands maintain their stability, invasive DNAs need sufficient energy to replace arm strands and a result is that it takes a longer time for disassembly.

Because longer invasive DNAs are still available for A_{12} and A_{24} aggregates due to a negligible increase in the background, they can still contribute to increase the disassembly kinetics of AuNP aggregates. So uranyl-induced disassembly kinetics of A_{12} and A_{24} aggregates were monitored with Inva-0, 2, 4, and 6 to find out whether there is any condition better than A_0 aggregates with Inva-6 at 40 mM NaCl 50 mM MES (pH 5.5) (Figure 3E and F). The integration ratio increases from Inva-0, 2 and Inva-4 were very similar and were slightly faster than Inva-6 for both A_{12} and A_{24} aggregates. However, most of the processes took about 20 min to saturate with the integration ratio increase from ranges 0.50−0.55 to 1.2−1.25, which is much slower than A_0 with Inva-6. These data show that an increase of the length of invasive DNAs could not improve the kinetics significantly for A_0 and A_{12} aggregates, and invasive DNA works the most effectively in A_0 aggregates rather than A_{12} and A_{24} aggregates probably due to the lower activation energy.

In the work described here, invasive DNA molecules are used to improve disassembly kinetics and thus sensing performance of the labeled sensing system. It relies on a detailed investigation of the role of invasive DNA in DNAzyme-AuNPs disassembly.[56] To minimize variables in the system, introducing DNA mismatches, less stable base pairs, or alkylguanine to lower T_m are all good alternate strategies and will be pursued in the future.

b. Sensitivity and Selectivity of Labeled DNAzyme-AuNP Colorimetric Sensor. Through the optimization process, we determined that A_0 aggregates have the best disassembly kinetics when Inva-6 was used as invasive DNA. This optimal construct was used to investigate the sensitivity of the UO_2^{2+}-dependent labeled DNAzyme-AuNP sensor, the plasmon resonance peak shift of AuNPs was monitored by UV−vis for 30 min, and the kinetics of the reaction is shown in Figure 4A based on the integration ratio between 490 to 540 nm and 550 to 700 nm at various UO_2^{2+} concentrations. The calibration curve based on the integration ratio of samples measured after 30 min of reaction is shown in Figure 4B. On the basis of the calibration curve, the detection limit of the labeled method for uranyl sensor is 50 nM and the calibration curve saturated at 2 μM. The image of color change is shown in Figure 4D.

To investigate the selectivity of the labeled DNAzyme-AuNP sensor, the plasmon resonance peak shift of AuNPs was monitored by UV−vis for 30 min and the integration ratio change was compared for various metal ions including UO_2^{2+} (Figure 4C). Only the sample with UO_2^{2+} shows a change in the plasmon shift, which means that the sensor only has a response with uranyl and not with other metal ions. The colors of the sensor solution in the presence of several metal ions (2 μM) are shown in Figure 4D.

Label-Free DNAzyme-AuNP Colorimetric Sensor. The scheme of the label-free method is illustrated in Figure 5. UO_2^{2+}-cleavable substrate−DNAzyme complex (complex) was first prepared separately and reacted with UO_2^{2+}. In the presence of UO_2^{2+}, substrate strand (39S) is cleaved and 10-mer ssDNA should be released, which can then be adsorbed onto AuNP to prevent the salt-induced aggregation. In the absence of UO_2^{2+}, however, the complex should remain and will not interact with AuNPs, resulting in AuNP aggregation due to the screening effect from NaCl and thus inducing color change of AuNPs from red to blue.

(74) Demers, L. M.; Oestblom, M.; Zhang, H.; Jang, N.-H.; Liedberg, B.; Mirkin, C. A. *J. Am. Chem. Soc.* **2002**, *124*, 11248–11249.

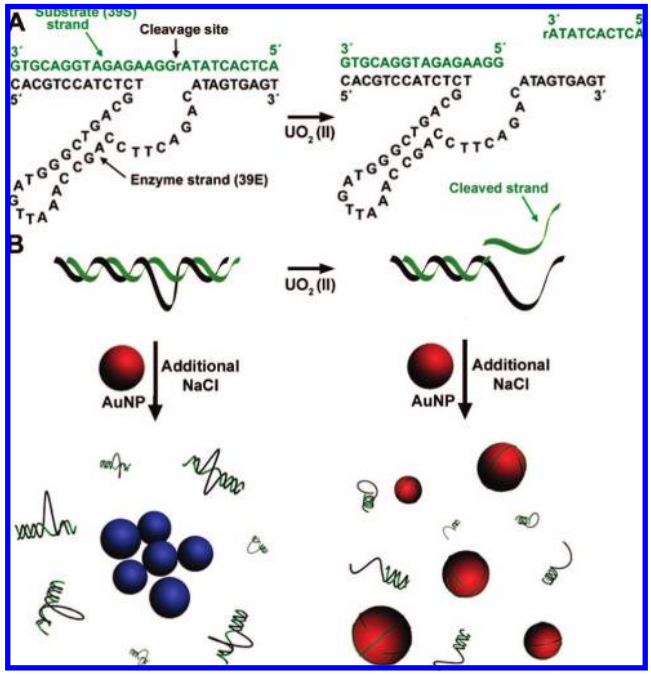

Figure 5. (A) Design and sequence of the label-free sensor (complex). After UO_2^{2+}-induced cleavage, 10 mer ssDNA is released which adsorbs on AuNP surface. (B) AuNP reaction in addition of UO_2^{2+} treated/untreated complex and additional NaCl. AuNPs aggregate in the absence of UO_2^{2+} but remain dispersed in its presence.

a. Stability of AuNPs upon Addition of NaCl and ssDNA. In most of the reported label-free colorimetric sensors, ssDNA is adsorbed onto AuNPs surface first and salt is added afterward to induce the color change. A 24-mer dsDNA is reported to be able to remain hybridized for about 10 min in the Au colloid without NaCl while introduction of a single mismatch will decrease the stability of dsDNA and thus cause dehybridization in 5 min.[52] DNAzymes, however, contain a large number of mismatches between the enzyme strand and substrate strand (Figure 5A), which causes dehybridization of the complex in seconds in the absence of NaCl.[75,76] So unlike previously reported studies, DNA solution has to be added to AuNP solution together with a sufficient amount of NaCl to keep the complex hybridized. In this case, because the stability of AuNPs is determined by the competition between the ssDNA adsorption on AuNP and electrostatic screening caused by NaCl which are introduced to AuNP solution at the same time, it is important to investigate whether DNA can still be adsorbed on AuNPs effectively and protect them in the presence of NaCl.

To investigate whether AuNPs can still be stabilized by ssDNA in the presence of NaCl, a 10 mer ssDNA was chosen as a model DNA strand to simulate the protection effect of the cleaved ssDNA from the substrate. Different amounts of 10-mer ssDNA in 300 mM NaCl, 10 mM MES (pH 5.5) were added to AuNP solution and their color change was monitored based on the extinction ratio between 522 and 700 nm (see Figure 6A) (see Supporting Information).

The concentration of NaCl in the final solution was 0.1 M. The extinction ratio (Abs_{522nm}/Abs_{700nm}) of AuNPs was linearly dependent on the amount of DNA at 0.1 M NaCl, suggesting that ssDNA can still stabilize AuNPs even though it is

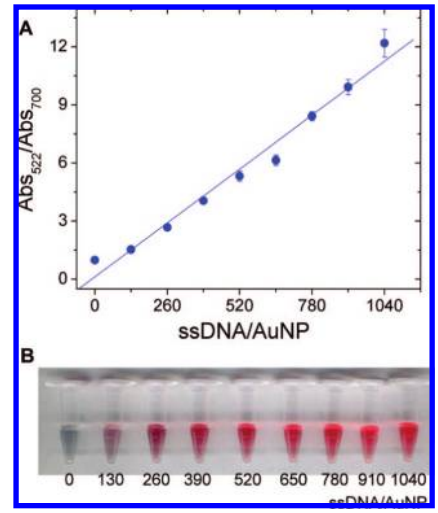

Figure 6. (A) Extinction ratio dependence on the number of 10 mer ssDNA per 13 nm AuNP. The stability of AuNP increases as more ssDNA exist per AuNP. (B) Color change of AuNPs with different ratio of DNA per AuNP.

introduced to AuNP solution with NaCl at the same time. The extinction ratio reached 11 when ~1000 equiv of ssDNA was used per AuNP. However, because the extinction ratio change from 1 to 5 is sufficient for detection, 500 equiv of ssDNA per AuNP was used in the following experiments because it could stabilize the AuNPs and make the color change from blue to red.

b. Quenching UO_2^{2+}-Dependent Cleavage Reaction by Shifting pH. Hybridization of substrate and enzyme strand was carried out at pH 5.5, where the UO_2^{2+}-dependent cleavage reaction occurs most efficiently.[39] Because the UO_2^{2+}-dependent cleavage reaction happens very quickly in several minutes, if the reaction cannot be effectively stopped during the measurements, significant error could occur, which makes the sensor impractical. Because biochemical investigation of this uranyl-specific DNAzyme showed that its activity is highly pH dependent, having the activity peak occurring around pH 5.5 with dramatic decrease of activity at either higher or lower pH,[70] we hypothesized that the DNAzyme might not be active at pH 8. Thus, to quench the reaction, a small amount of concentrated TRIS (2-amino-2-(hydroxymethyl)propane-1,3-diol) base solution was added to the solution containing the complex to shift pH from 5.5 to around 8.

UV−vis spectroscopy was used to monitor the quenching effect of uranyl-induced cleavage reaction using TRIS base solution (see Figure 7A). When the complex was added to AuNP solution without addition of uranyl, an extinction ratio of ~1.4 was observed, suggesting AuNP aggregation. On the other hand, when the complex was treated with 500 nM uranyl for 6 min, an extinction ratio of ~4 was observed, indicating AuNP dispersion. When the reaction was quenched by adding TRIS base solution after 1 min of uranyl-induced reaction followed by addition to AuNP solution, an extinction ratio of ~2.2 was observed, suggesting partial AuNPs dispersion. This means that the uranyl-induced cleavage ratio has been stopped by the quenching reaction. To make sure that the quenching reaction was complete and no further uranyl-induced reaction happened afterward, a control experiment was performed that had 5 min interval between uranyl-induced cleavage reaction (1 min) and mixture in AuNP solution. It was shown that even though there were 5 min of interval between quenching and mixture with

(75) Liu, J.; Lu, Y. *Anal. Chem.* **2003**, *75*, 6666–6672.
(76) Wernette, D. P.; Mead, C.; Bohn, P. W.; Lu, Y. *Langmuir* **2007**, *23*, 9513–9521.

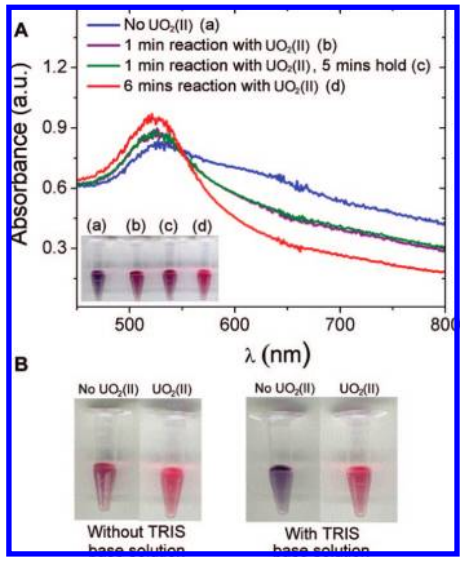

Figure 7. (A) Quenching efficiency of label-free sensor by shifting the pH of the solution from 5.5 to 8. AuNPs are aggregated in the absence of UO_2^{2+} (blue curve) but remain dispersed after 6 min of reaction with 2 μM UO_2^{2+} (red curve). AuNPs show less amount of disassembly after 1 min of reaction with 2 μM UO_2^{2+} and quenching (purple curve). No further disassembly of AuNP aggregates after 5 min of holding in between quenching and AuNP addition (green curve) shows that quenching efficiency is very high and quick. The color change of each sample is also shown in the inset. (B) Color change difference before (upper) and after (lower) addition of TRIS base solution. Concentration of uranyl is 2 μM.

AuNP, there was no further uranyl-induced cleavage reaction. This result indicates the TRIS base solution could quench the reaction very effectively and in time. Furthermore, it turned out that TRIS also helps to aggregate AuNPs more effectively and thus helps to lower the background signal (Figure 7B).

c. Sensitivity and Selectivity of Label-Free Colorimetric Sensor for UO_2^{2+}. To check the sensitivity of UO_2^{2+} dependent label-free colorimetric sensor, the plasmon resonance peak shift of AuNPs was monitored by UV−vis and the extinction ratio between 522 and 700 nm was compared at various UO_2^{2+} concentrations (Figure 8A). The detection limit was determined to be 1 nM and the linear fitting range was from 1 to 100 nM. The calibration curve was saturated at 700 nM, which is similar to the fluorescence-based uranyl sensor.[39] Because the UO_2^{2+}-dependent cleavage reaction was made in concentrated DNAzyme solution in optimized conditions, followed by the addition of AuNP, the UO_2^{2+}-dependent cleavage reaction can happen very efficiently, which helps to keep high sensitivity. Furthermore, as reacted DNA solution containing NaCl is added to AuNP solution after quenching, the color of AuNP solution change occurs immediately and does not change much afterward.

In the low concentration range (Figure 8A), the extinction ratio increases with increasing concentration of uranyl until it saturates ~700 nM, beyond which the ratio decreases with increasing uranyl concentrations. This "bell-shape" metal-dependent curve appears to have originated from uranyl-dependent DNAzyme activities,[39] and similar curves have been reported in other DNAzymes.[32−34] The image of color change is shown in Figure 8B. Because a UO_2^{2+}-dependent cleavage reaction can easily be quenched by shifting the pH from 5.5 to 8, it might be possible to tune the dynamic range simply by changing the reaction time.

To investigate the selectivity of label-free sensor, several metal ions including uranyl were added to sensor solution and their color changes are shown in Figure 8C. The result clearly

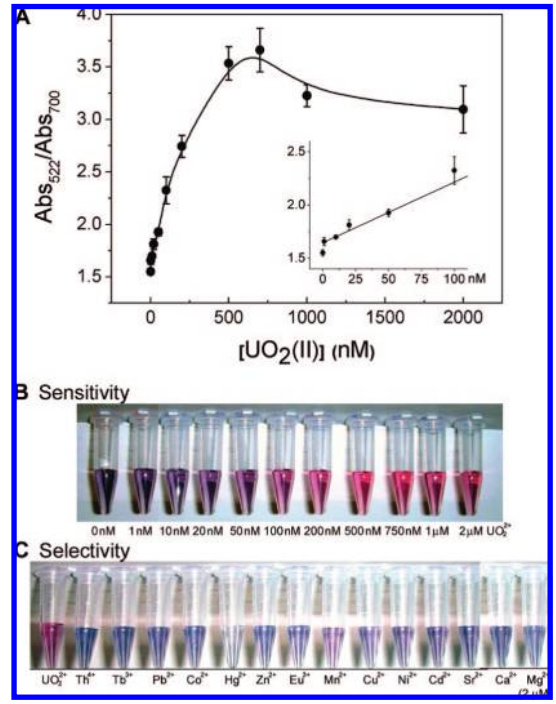

Figure 8. (A) Calibration curve of label-free sensor. The sensor has a detection limit of 1 nM. (B) Color change of AuNP solution with different concentration of UO_2^{2+} in the solution. (C) Color change of AuNP solution with various metal ions including UO_2^{2+} (2 μM).

Table 1. Comparison between Labeled and Label-Free Colorimetric UO_2^{2+} Sensors

sensors	labeled sensor	label-free sensor
Detection range	50 nM-2 μM	1 nM-700 nM
Detection limit	50 nM	1 nM
Linear range	50−500 nM	1−100 nM
Saturation point	2 μM	700 nM
Working time	30 min	6 min
Working temperature	Room temperature	Room temperature
Operation step	1 step	3 steps
Quenching	No	Possible (by shifting pH)
Std. Dev.	~10% of the signal change when saturated	~10% of the signal change when saturated
Color Change	Purple to red (in the presence of analyte)	Red to blue (in the absence of analyte)
Type	Turn on	Turn off
Stability of AuNPs	Stable	Less stable

shows that the sensor only has a response in the existence of uranyl, indicating that the sensor has excellent selectivity.

Comparison between Labeled and Label-Free Based Colorimetric Sensors. Because both colorimetric methods have been demonstrated to successfully detect uranyl, it gave us the opportunity to compare the properties of both sensors using the same DNAzyme and AuNPs.

In terms of performance of sensors, as labeled sensing method depends on UO_2^{2+}-induced cleavage of substrate strands in aggregated state and the release of AuNP aggregates, certain amount of UO_2^{2+} and time is necessary for the cleavage to complete, which could explain the relatively higher detection limit (50 nM) and slower kinetics (30 min). On the other hand, as label-free sensor allows UO_2^{2+}-based cleavage reaction to occur separately without AuNPs and AuNPs solution is added afterward for signaling, the cleavage could be completed with less amount of UO_2^{2+} and less time, resulting in a relatively

lower detection limit (1 nM) and shorter sensing time (6 min). Despite this difference, both sensors have detection limits that are much lower than the maximum contamination level defined by the U.S. EPA (130 nM)[71] and have excellent selectivity over other metal ions. Furthermore, both sensors operate at room temperature.

For preparation and handling of sensors, it takes more time and effort to prepare the labeled sensor, but the labeled sensor is more convenient to handle once the sensor is prepared, as sensing can be carried out through one step of addition of uranyl. On the other hand, the label-free sensor can be easily prepared, but requires three processing steps, uranyl addition, quench, and AuNP addition, for detection. In doing so, the label-free method contains many more variables that are uncertain for on-site and real-time detection. Therefore, for practical applications, it is desirable for professionals to spend more time and efforts to prepare the sensors in a laboratory to minimize steps for on-site operation; the more processing steps for on-site operation, the more likely errors could occur, especially when used by nonprofessional operators.

In addition, because the AuNPs in labeled sensor are modified with thiolate oligonucleotides, they are much more stable than those in the label-free sensor and thus can be stored for a long time and used under a variety of conditions. In contrast, the AuNPs used in label-free sensors are much less stable and requires much narrow range of conditions such as ionic strength to operate. The stability of AuNP is very important for practical applications because it is the key ingredient for the sensor. In addition, labeled system could be easily incorporated into lateral flow devices under a variety of conditions,[59] while a much more carefully controlled condition may be required if label-free AuNPs were to be used. Finally, the labeled method resulted in a turn-on sensor, going from purple AuNP aggregates into red disassembled AuNPs upon addition of uranyl, whereas the label-free DNAzyme-AuNP sensor is a turn-off sensor; the red AuNPs remains red in the presence of uranyl but changes to blue in the absence of uranyl. Turn-on sensors are preferred as they are much less vulnerable to false positive signals due to interfering metal ions, other species, or conditions. Furthermore, the labeled methods can be designed as turn-off sensors,[23,55] demonstrating versatility in sensor design for the labeled system.

In conclusion, uranyl specific colorimetric sensors using gold nanoparticles and uranyl selective DNAzyme were prepared by both labeled and label-free methods and the general properties of the two colorimetric sensors were compared in various aspects. The labeled sensor is simpler to use as it requires a one-step process once the sensor is prepared and is more versatile as DNA functionalized on AuNPs provides stability and turn-on sensing. On the other hand, the label-free sensor has better sensitivity, shorter operation time and lower costs. Despite the difference, both sensors have detection limits lower than the maximum contamination level defined by the U.S. EPA (130 nM), have excellent selectivity over other metal ions, and operate at room temperature. If operation requires a very low detection limit, the label-free should be a better choice. When detection limit is adequate, such as in the case of uranyl sensing, the labeled method should be used due to turn-on sensing, and high stability of the system that allows operation under a variety of conditions.

Experimental section

Oligonucleotide and Reagents. All oligonucleotides were purchased from Integrated DNA Technologies Inc. (Coralville, IA). DNAzyme strand (39E) and both substrate strands (39S-L for labeled DNAzyme-AuNP sensor and 39S for label-free) were purified by HPLC by the company while the arm strands with thiolate modifications and invasive DNA strands were standard desalted. $HAuCl_4$ (99.999%), sodium citrate dehydrate (99+%) were purchased from Aldrich and used without further purification.

Labeled Sensor. a. Preparation and Functionalization of AuNPs. Gold nanoparticles (13 nm diameter) were synthesized by reduction of $HAuCl_4$ by sodium citrate, and the AuNP-DNA conjugate were prepared following the published protocol.[44] To activate thiol modification on Arm (5′) strand, 9 μL of 1 mM Arm (5′) strand, 1 μL of 500 mM pH 5.5 MES buffer, and 1.5 μL of 10 mM tris (2-carboxyethyl)phosphine hydrochloride (TCEP) solution were mixed in a microcentrifuge tube and kept for an hour. In a separate tube, a parallel experiment was done with Arm (3′) strand to activate thiol modification on Arm (3′) strand.

At the same time, two scintillation vials were incubated in fresh 10 M NaOH solution for an hour and then rinsed with distilled water for several times and then with Millipore water (18 MΩ) for copious times to prevent AuNP sticking on the surface of glass vials.

To attach AuNP with Arm (5′) DNA strand, 3 mL of 13 nm AuNP solution was placed in one scintillation vial and activated 9 μL Arm (5′) strand was added and left overnight in a dark place for reaction after gentle shaking. In the other scintillation vial, another 3 mL of 13 nm AuNP solution was mixed with activated 9 μL Arm (3′) strand and then was treated in the same way. Three-hundred microliters of 1 M NaCl and 15 μL of 500 mM TRIS-acetate buffer (pH 7.6) was added on the next day and again kept in a dark place overnight after gentle shaking.

To prepare labeled sensor, DNA functionalized AuNPs were first purified to remove free DNA in AuNP solution. Five-hundred microliters of AuNP functionalized with Arm (5′) strand and same amount of AuNP functionalized with Arm (3′) strand were placed in two 1.5 mL microcentrifuge tubes, respectively, and were centrifuged at 16 110*g* for 15 min. After that, supernatant in both solutions was replaced with fresh 500 μL of 100 mM NaCl, 50 mM MES (pH 5.5) solution. After the purification process was repeated, the supernatant was replaced with 250 μL of 300 mM NaCl, 50 mM MES (pH 5.5) buffer. After mixing two AuNP solutions, 10 μL of 10 μM elongated substrate strand (39S-L), and 20 μL of 10 μM enzyme strand (39E) were added and annealed from 55 °C to room temperature for about 1 h. The color of AuNP solution changed from red to purple which shows that DNA directed AuNPs assembly happened. The AuNPs aggregates were centrifuged by a microcentrifuge for about a minute and the supernatant was replaced with 120 μL of 300 mM NaCl, 50 mM MES (pH 5.5) solution to remove free DNA (39S-L and 39E) in the sensor solution.

b. Activity Assays. To prepare aggregates containing ^{32}P-labeled substrate, ~0.1% of ^{32}P-labeled substrates (in respect to the total substrate amount) were added, while keeping other conditions the same. ^{32}P-labeled aggregates were added to a solution with 1 μM UO_2^{2+}, 300 mM NaCl and 50 mM MES, pH 5.5. Aliquots were taken out at designated time points and quenched in a solution containing 8 M urea and 200 mM EDTA. The quenched aliquots were heated at 60 °C to fully release substrate strands from aggregates and then loaded to 20% denaturing polyacrylamide gel. ^{32}P-labeling and procedures for single-turnover solution phase activity assays were the same as reported elsewhere.[72]

c. Uranyl Detection. To detect uranyl using labeled sensor, 381 μL of 50 mM MES buffer (pH 5.5), 4.5 μL of 0.2 mM Inva-6 (5′), 4.5 μL of 0.2 mM Inva-6 (3′) were mixed and 60 μL of sensor solution in 300 mM NaCl, 50 mM MES (pH 5.5) was added just before UV−vis measurement. The concentration of invasive DNA is 2 μM in the final solution. Uranyl was added 1 min after the measurement has started and the whole reaction was made for 30 min. Calibration curve was made based on the data collected on

the 31st minutes after 30 min of reaction. Uranyl acetate stock solution was used as uranyl source.

Label-Free Sensor. a. AuNPs Stabilized by ssDNA in the Presence of NaCl. Different amount (from 0 to 8 μL) of 10 mer DNA (5′-CAT GCT ACT G-3′, 100 μM) was added into 70 μL of 300 mM NaCl, 10 mM MES buffer solution (pH 5.5) in a 0.6 mL microcentrifuge tube. A mixture of 1.19 μL of 500 mM TRIS base solution and appropriate amount of Millipore water was added to make the total volume as 134 μL. After vortex, 76 μL 10 nM Au nanoparticles (13 nm) were added and the surface plasma absorption was collected by UV−vis spectra.

b. Sensor Preparation and Uranyl Detection. UV−vis was used to check the exact concentration of 39E and 39S strands. This process is very important because a very small number of unhybridized ssDNA can still stabilize AuNP and increase the background. Based on the measured concentration, 4 μL of 100 μM 39S strand and equal amount of 39E strand were mixed in 70 μL 300 mM NaCl, 10 mM MES buffer solution (pH 5.5) in a 0.6 mL microcentrifuge tube. After vortex, sample was heated up to 80 °C and cooled down to room temperature in one hour and a half. Hybridization solution can be multiplied by preparing in large scale in volume. After that, 77 μL of solution containing hybridized DNAzyme and enzyme strand was transferred into a new tube and cleaved by uranyl for 6 min. To quench UO_2^{2+}-dependent cleavage reaction, a mixture of 1.19 μL of 500 mM TRIS base solution and 56 μL Millipore water was added to the same tube and the tube was vortexed quickly which in result shifts the pH from 5.5 to 8. Seventy-six microliters of 10 nM Au nanoparticles (13 nm) was transferred to the tube containing DNA. The solution will show a color change corresponding to the concentration of uranyl in the solution. The color change can be monitored by eye or by plasmon peak shift in UV−vis spectra.

Acknowledgment. This work has been supported by the Office of Science (BER), U.S. Department of Energy, Grant No. DE-FG02-08ER64568, the U.S. National Science Foundation (CTS-0120978, DMR-0117792, and DMI-0328162), and National Institutes of Health (ES016865).

Note Added after ASAP Publication. The version of this paper published on October 7, 2008, contained an error in Figure 2. The version published on October 22, 2008 contains the corrected Figure 2.

Supporting Information Available: Data on melting curves of A_0 and A_{12} aggregates at 30 and 100 mM NaCl and uranyl-induced disassembly of A_{12} aggregates in the presence of 30 mM NaCl at room temperature. The reason for using the integration ratio method for labeled and the extinction ratio method for label-free systems. This material is available free of charge via the Internet at http://pubs.acs.org.

JA803607Z